
Molecular Modeling of Hydrogen Bonding Fluids: New Cyclohexanol Model and Transport Properties of Short Monohydric Alcohols

Thorsten Merker, Gabriela Guevara-Carrión, Jadran Vrabec,
and Hans Hasse

Institut für Technische Thermodynamik und Thermische Verfahrenstechnik,
Universität Stuttgart, D-70550 Stuttgart, Germany
vrabec@itt.uni-stuttgart.de

1 Introduction

Currently, molecular modeling and simulation gains importance for the prediction of thermophysical properties of pure fluids and mixtures, both in research and industry. This is due to several reasons: Firstly, the predictive power of molecular models allows for results with technically relevant accuracy over wide range of state points that is superior to classical methods. Secondly, a given molecular model provides access to the full variety of thermophysical properties, such as thermal, caloric, transport or phase equilibrium data. Finally, through the advent of cheaply available powerful computing infrastructure, reasonable execution times for molecular simulations can be achieved which are of particular importance for industrial applications. Molecular modeling and simulation are based on statistical thermodynamics which directly links the intermolecular interactions to the macroscopic thermophysical properties. That sound physical background also supports the increasing acceptance compared to classical phenomenological modeling.

Modeling thermophysical properties of hydrogen bonding systems remains a challenge. Phenomenological models often fail to describe the interplay between the energetics of hydrogen bonding and its structural effects. Molecular force field models, however, are much better suited for solving that task as they explicitly consider this interplay. Most of the presently available molecular models use crude assumptions for the description of hydrogen bonding which can, for instance, be simply modeled by point charges eccentrically superimposed to Lennard-Jones (LJ) sites. One benefit of this simple modeling approach for hydrogen bonding is the comparably small number of adjustable model parameters. Furthermore, the approach is compatible with numerous

LJ based models from the literature and it can successfully be applied to mixtures. This simple modeling approach emerged to be fruitful in many ways, although many of the molecular models proposed in the literature lack in the quantitatively sound description of thermophysical properties. The aim of this project is to tackle that problem and to show that a thorough modeling and parameterization does indeed yield quantitatively correct results.

Molecular models which accurately describe vapor-liquid equilibria over the full temperature range usually exhibit a good predictive power throughout the whole fluid region. The molecular model for ethanol developed in the first period of the MMHBF project [1] has these characteristics and excellently performed in the prediction of vapor-liquid equilibrium properties of mixtures, i.e. Henry's law constants [2, 3]. To study the chosen modeling approach also regarding other strongly associating fluids, a new molecular model for formic acid [4] was developed earlier in the present MMHBF project [5]. Formic acid is the simplest carboxylic molecule and has exceptional thermophysical properties due to its ability to act both as hydrogen bond donor and acceptor. Since both hydrogen atoms of formic acid can act as proton donors and both oxygen atoms provide proton acceptance, four unlike hydrogen bond types yield the basis for a complex self-association which is the reason for its exceptional thermophysical behavior. The developed molecular model for formic acid also excellently describes the vapor-liquid equilibrium properties.

The Collaborative Research Centre 706 (SFB706) offers attractive applications for the present work. There, novel octahedral molecular sieves for the heterogeneously catalyzed selective oxidation of cyclohexane are investigated. Supercritical fluids and carbon dioxide-expanded liquids are used as innovative reaction media. For a rational planning of catalytic experiments and process design, especially at higher pressures, reliable thermodynamic data are needed. Most groups used in the past nitrogen instead of oxygen to predict the phase behavior of the reacting system. For predictive applications, e.g. the Peng-Robinson equation of state has been used, as true experimental vapor-liquid equilibria of binary mixtures containing oxygen for this reaction system are rare, especially at elevated temperatures and pressures. Molecular modeling and simulation is an excellent approach to bypass the lack of experimental data. Cyclohexanol is the central component in this reaction system. Therefore, a new molecular model for cyclohexanol was developed in the present period of the MMHBF project with the aim to accurately describe the vapor-liquid equilibrium. Cyclohexanol is the largest hydrogen bonding molecule which was modeled within the present project to date.

Another interesting application of molecular modeling and simulation are the transport properties of liquids. Due to the complexity of the involved physical mechanism, only molecular methods offers promising predictive approaches to this problem, especially for hydrogen bonding fluids. In this project, the self-diffusion coefficient of pure methanol and ethanol as well as in the mixture of both components was regarded.

Two fundamentally distinct methods for calculating transport properties by molecular dynamics simulation are available. The equilibrium methods (EMD), using either the Green-Kubo formalism or the Einstein relations, determine the time dependent response of a fluid system to spontaneous fluctuations. With non-equilibrium molecular dynamics (NEMD), on the other hand, the system response to an externally applied perturbation is analyzed. The later method was developed in order to increase the signal to noise ratio and to improve statistics and convergence. Both methods exhibit different advantages and disadvantages, but are comparable in efficiency, as shown, e.g. by Dysthe et al. [6].

The present work is based on rigid, united-atom type Lenard-Jones based models with superimposed point charges for methanol and ethanol developed earlier [4, 2]. It should be pointed out that these models were optimized using experimental data of vapor pressure and saturated liquid density. The goal of this study is to demonstrate the ability of molecular models, adjusted to these vapor-liquid equilibrium data only, to accurately predict transport properties.

Results of this work are consistently published in peer-reviewed international journals. The following publications contribute to the present project:

- T. Merker, J. Vrabec and, H. Hasse: Comment on “An optimized potential for carbon dioxide” [J. Chem. Phys. 122, 214507 (2005)]. J. Chem. Phys., submitted (2008).
- T. Merker, J. Vrabec and, H. Hasse: Molecular models for carbon dioxide and cyclohexanol. In preparation
- G. Guevara-Carrión, C. Nieto-Draghi, J. Vrabec and, H. Hasse: Prediction of the Transport Properties for Short Monohydric Alcohols: Methanol, Ethanol and their Binary Mixture. In preparation

This report is organized as follows: Firstly, the new molecular model for cyclohexanol is introduced. Subsequently, the self-diffusion coefficient of methanol and ethanol is presented. Finally, remarks on computational details are given.

2 Molecular Model for Cyclohexanol

A new cyclohexanol model was developed based on quantum mechanical calculations and optimized using experimental vapor pressure, bubble density and heat of vaporization. As the complexity of a molecular model determines the required computing time in molecular simulation, it was attempted to find an efficient solution balancing accuracy and simplicity. A rigid model with seven LJ sites plus one point quadrupole and three point charges was chosen. The assumption of rigidity was chosen as the cyclohexane ring predominantly forms the energetically favorable chair-conformation.

The geometric parameters of the molecular model were taken directly from quantum mechanical calculations. For this purpose, initially a geometry optimization was performed with the GAMESS (US) package [7], employing the

Table 1. Coordinates and parameters of the LJ sites and the point charges in the principal axes system of the new molecular model for cyclohexanol. Bold characters indicate represented atoms

Interaction Site	x Å	y Å	z Å	σ Å	ε/k_B K	q e
CH₂(1)	-2.16883	-0.55100	0	3.412	102.2	—
CH₂(2)	-1.30893	0.44982	-1.57594	3.412	102.2	—
CH₂(3)	0.56919	-0.40155	-1.56168	3.412	102.2	—
CH₂(4)	0.56919	-0.40155	1.56168	3.412	102.2	—
CH₂(5)	-1.30893	0.44982	1.57594	3.412	102.2	—
CH	1.06798	0.33582	0	3.234	60.0	0.256184
OH	2.45979	0.00085	0	3.150	85.1	-0.638767
H-O	2.50948	-0.97164	0	—	—	0.382583

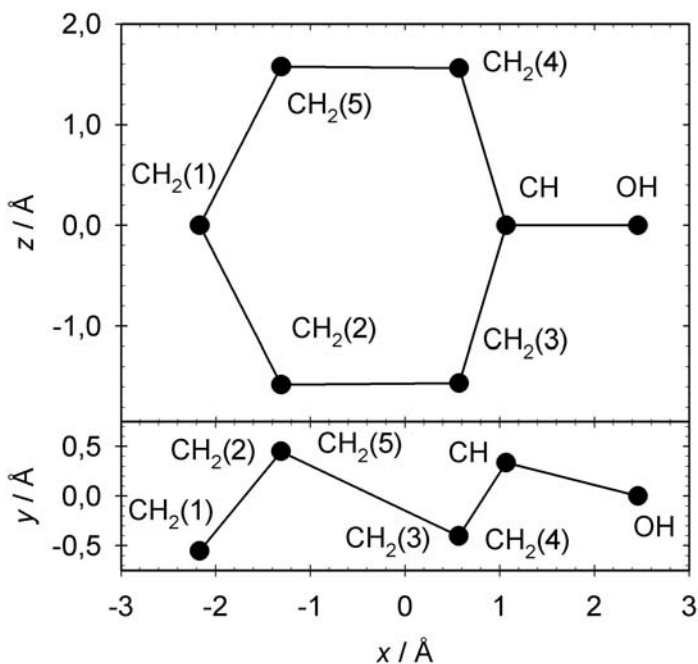


Fig. 1. Coordinates of the LJ sites for the present cyclohexanol model

Hartree-Fock method and the basis set 6-31G. For the quantum chemical calculations, the symmetry of the molecule was exploited and only half of it was regarded. A LJ site was located exactly at all resulting nuclei positions, except for the hydrogen atom. The ethyl and methyl group was modeled by a single LJ site, i.e. the united-atom approach was used. The coordinates of the seven LJ sites are given in Table 1 and in Figure 1.

Table 2. Orientation and moment of the point quadrupole placed in the center of mass of the new molecular model for cyclohexanol. Orientations are defined in standard Euler angles, where φ is the azimuthal angle with respect to the $x - z$ plane and θ is the inclination angle with respect to the z axis

Site	x	y	z	φ	θ	Q
	Å	Å	Å	deg	deg	
Quadrupole	0	0	0	90	90	0.795561 B

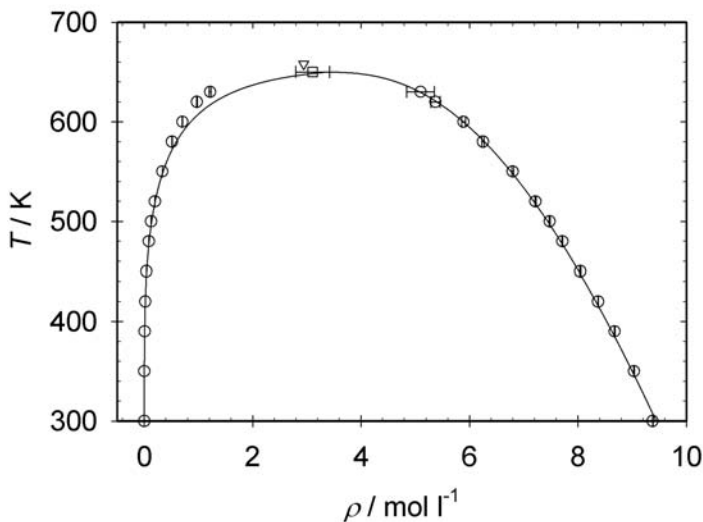


Fig. 2. Saturated densities of cyclohexanol: \circ , present simulation data; —, experimental data [8]; ∇ , critical point derived from simulated data; \square , experimental critical point [8]

A subset of the parameters for the LJ sites, the point quadrupole and the point charges were optimized to fit correlations of experimental saturated liquid density and vapor pressure of pure cyclohexanol [8] in the range from 325 to 635 K. As a starting set for optimization, LJ parameters for the CH_2 site and electrostatic parameters for the point quadrupole were taken from a recently developed cyclohexane model. The remaining LJ parameters for the CH and OH group and the point charges were taken from Schnabel et al. [3]. During the present optimization, the LJ parameters of the CH_2 sites, the point charges and the point quadrupole were adjusted. The optimization followed the procedure presented by Stoll [9].

Vapor-liquid equilibria of the new cyclohexanol model are presented together with experimental data [8] in Figures 2 to 4 and in Table 3. The agreement between the molecular model and the experimental data is good. The mean unsigned errors in vapor pressure, bubble density and heat of va-

Table 3. Vapor-liquid equilibria of cyclohexanol: simulation results (sim) are compared to experimental data (DIPPR) [8] for vapor pressure, saturated densities and enthalpy of vaporization. The number in parentheses indicates the statistical uncertainty in the last digit

T K	p_{sim} MPa	p_{DIPPR} MPa	ρ'_{sim} mol/l	ρ'_{DIPPR} mol/l	ρ''_{sim} mol/l	$\Delta h^{\text{v}}_{\text{sim}}$ kJ/mol	$\Delta h^{\text{v}}_{\text{DIPPR}}$ kJ/mol
300	—	—	9.378(3)	9.440	—	—	—
350	0.002(4)	0.003	9.032(8)	9.000	0.00076(0)	54.06(9)	56.05
390	0.023(2)	0.022	8.674(6)	8.625	0.00704(0)	49.96(3)	51.16
420	0.062(3)	0.065	8.371(4)	8.328	0.01807(2)	46.71(3)	47.31
450	0.145(6)	0.159	8.043(6)	8.014	0.04062(6)	43.39(3)	43.27
480	0.31 (1)	0.331	7.71 (1)	7.677	0.0842 (2)	40.03(4)	39.01
500	0.47 (2)	0.504	7.48 (1)	7.439	0.1267 (3)	37.80(3)	36.02
550	1.23 (3)	1.202	6.80 (2)	6.762	0.335 (1)	31.42(4)	27.81
600	2.43 (2)	2.394	5.89 (3)	5.883	0.704 (4)	23.92(6)	17.88
620	3.11 (5)	3.046	5.37 (9)	5.396	0.972 (8)	19.78(7)	12.92

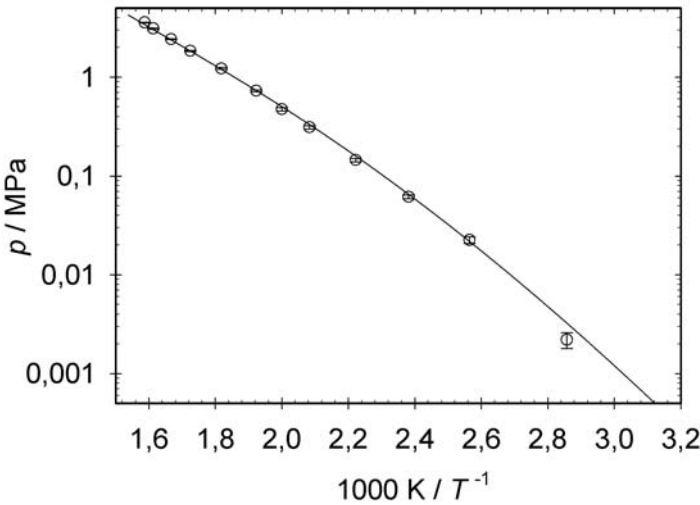


Fig. 3. Vapor pressure of cyclohexanol: \circ , present simulation data; —, experimental data [8]

porization are 4.1, 0.4, and 13.4 %, respectively, in the temperature range from 325 to 635 K, which is about 50 to 97 % of the critical temperature. The seemingly high unsigned error in the heat of vaporization is due to the lack of experimental data for cyclohexanol. In fact, the only available experimental data for the heat of vaporization are at low temperatures, where the present molecular model shows a very good agreement, cf. Figure 4.

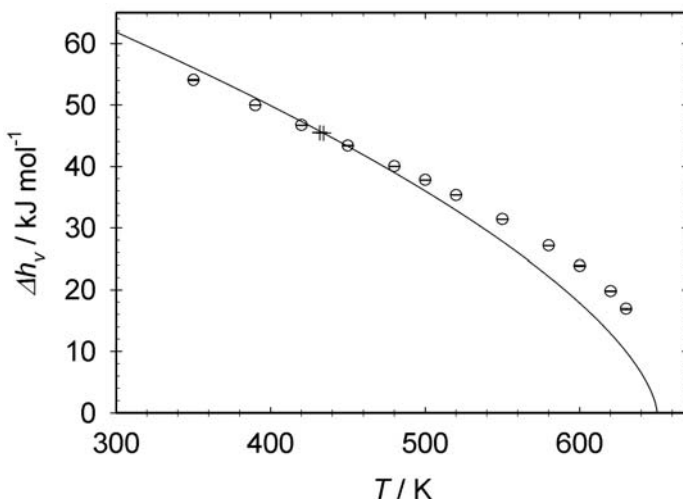


Fig. 4. Heat of vaporization of cyclohexanol: ○, present simulation data; —, predicted experimental data [8]; ⊕, experimental data [8]

3 Transport Properties

Dynamic properties can be obtained from EMD simulations by means of the Green-Kubo equations [10, 11]. These equations are a direct relationship between a transport coefficient and the time integral of an autocorrelation function of a particular microscopic flux in a system at equilibrium. This method was used in this work to calculate the self-diffusion coefficient.

3.1 Diffusion Coefficient

The self-diffusion coefficient D_i is related to the mass flux of single molecules within a fluid. Therefore, the relevant Green-Kubo formula is based on the individual molecule velocity autocorrelation function as follows

$$D_i = \frac{1}{3N} \int_0^\infty dt \langle \mathbf{v}_k(t) \cdot \mathbf{v}_k(0) \rangle, \quad (1)$$

where $\mathbf{v}_k(t)$ is the center of mass velocity vector of molecule k at some time t , and $\langle \dots \rangle$ denotes the ensemble average. Eq. (1) is an average over all N molecules in a simulation, since all contribute to the self-diffusion coefficient.

3.2 Simulation Results

The self-diffusion coefficient of pure methanol and ethanol was predicted at atmospheric pressure in the temperature range between 200 and 340 K. Present

numerical data are given in Table 4. Figure 5 shows the self-diffusion coefficient for both alcohols as a function of temperature. The statistical error of the simulation data was estimated to be in the order of 1%.

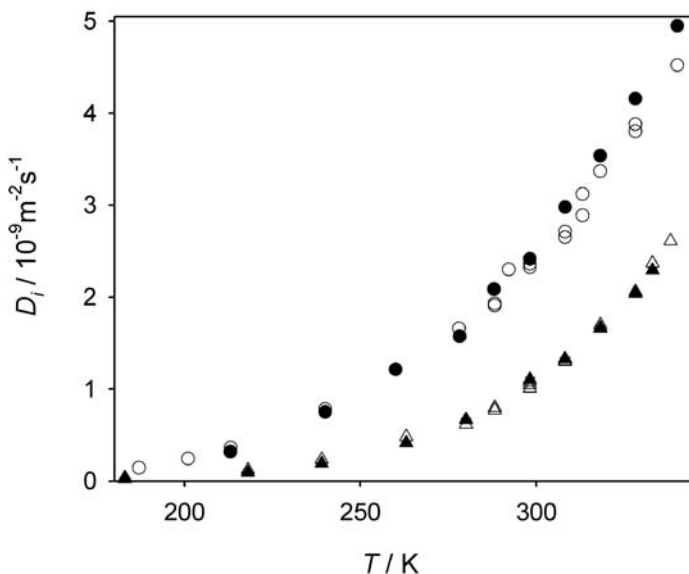


Fig. 5. Temperature dependence of the self-diffusion coefficient at 0.1 MPa. Present simulation results for methanol (●) and ethanol (▲) are compared to experimental data (○) [12, 13, 14, 15, 16] and (△) [12, 13, 14, 15, 17]. Simulation error bars are within symbol size

Table 4. Density and self-diffusion coefficient of pure liquid methanol and ethanol at 0.1 MPa from present molecular dynamics simulations. The number in parenthesis indicates the statistical uncertainty in the last digit

T	ρ	D_i	T	ρ	D_i
K	mol/l	$10^{-9} \text{m}^2/\text{s}$	K	mol/l	$10^{-9} \text{m}^2/\text{s}$
Methanol			Ethanol		
213	27.02	0.174(4)	239	18.11	0.192(6)
240	26.22	0.549(7)	263	17.74	0.415(9)
260	25.63	1.01 (1)	280	17.44	0.67 (1)
278.15	25.14	1.57 (1)	298.15	17.08	1.11 (2)
288	24.81	2.09 (2)	308.15	16.88	1.33 (2)
298.15	24.51	2.41 (2)	318.15	16.65	1.71 (1)
318.15	23.91	3.47 (2)	328.15	16.45	2.04 (2)
328.15	23.58	4.16 (2)	333	16.31	2.30 (2)
340.15	23.21	4.95 (3)	—	—	—

The self-diffusion coefficient of methanol shows a good agreement with the experimental values. Below ambient temperature, the mobility of the model molecules decreases more rapidly than in real methanol. Hence, the self-diffusion coefficient from simulation is underestimated by about 5%. At temperatures above 298 K the self-diffusion coefficient is overestimated by up to 12% at 340 K. However, the significant scatter of the experimental data should be noticed.

The self-diffusion coefficient of ethanol shows an excellent agreement with the experimental data. The predicted data also reproduce the temperature dependence correctly over the whole regarded temperature range from 239 to 333 K. Deviations are on average 5%.

Selected normalized velocity autocorrelation function (VACF) of methanol and ethanol are shown in Figure 6. In agreement with findings in the literature, VACF may have two minima at short times ($t < 1$ ps) [18]. At low temperatures and high densities, the VACF decrease rapidly and assume negative values. After this first minimum, the VACF increase slightly to drop again into a deeper minimum, for methanol, or to a higher minimum, in the case of ethanol. Beyond the second minimum, the VACF converge to zero following a characteristic path. The observed negative values of the VACF are related to backscattering collisions, also known as cage-effect, which governs short time dynamics. Michels and Trappeniers [19] attribute this phenomenon to the formation of “bound states” since this effect can only be observed for molecular models that include attractive forces.

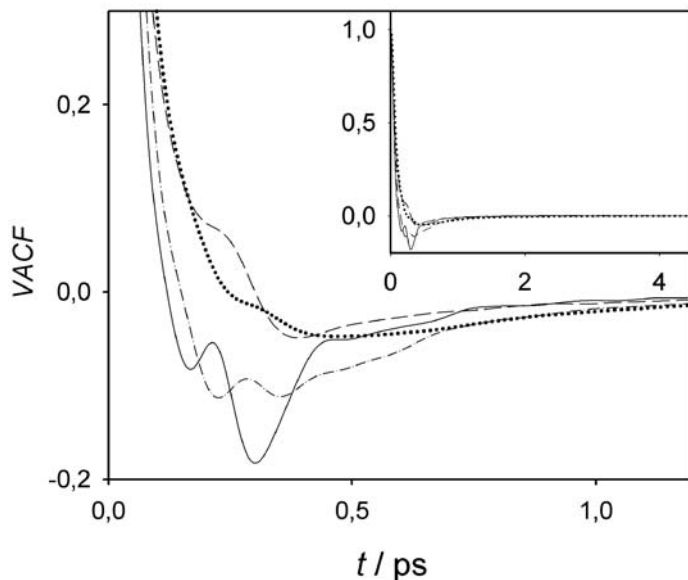


Fig. 6. Velocity autocorrelation functions at 0.1 MPa of methanol at 180 K (—) and 340 K (---) as well as of ethanol at 173 K (- · -) and 333.15 K (···)

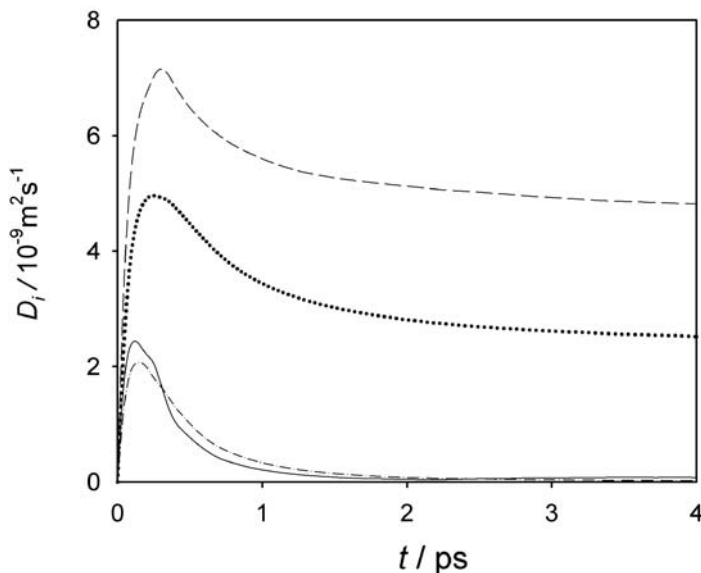


Fig. 7. Integral of the velocity autocorrelation functions at 0.1 MPa of methanol at 180 K (—) and 340 K (---) as well as of ethanol at 173 K (— · —) and 333.15 K (····)

For increasing temperatures at atmospheric pressure, where the density is lower, molecular collisions are less frequent and the depth of the minima is gradually reduced until they almost disappear, cf. Figure 6. As can be assumed, the VACF decay faster at lower temperatures, which is clearly visible in Figure 6. Moreover, the initial drop of the VACF of methanol occurs earlier than the corresponding VACF for ethanol. Thus, methanol VACF exhibit a more pronounced backscattering than those of ethanol, particularly at low temperatures approaching its melting temperature ($T_m = 175.37$ K) [20]. Note that the absolute minimum of the ethanol velocity autocorrelation function occurs in between the two minima of the methanol VACF.

Figure 7 shows the behavior of the integrals of the VACF given by Eq. (1). It can be observed that all VACF converge to their final value after less than 4 ps, i.e. no long time tail contributes significantly to the value of the self-diffusion coefficient at the regarded state points.

The changes of the self-diffusion coefficient of methanol and ethanol in that binary mixture were predicted at 298.15 K and 0.1 MPa for the entire composition range. Numerical results are presented in Table 5. Fig. 8 shows the self-diffusion coefficient of methanol and ethanol as a function of the methanol mole fraction in the mixture. As can be observed, there is a very good agreement between the present self-diffusion coefficients and the experimental data

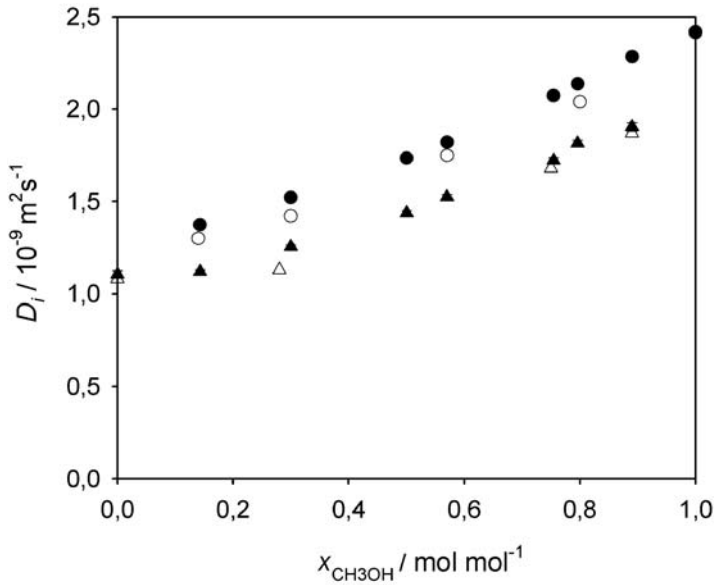


Fig. 8. Composition dependence of the self-diffusion coefficient for the mixture methanol + ethanol at 298.15 K and 0.1 MPa. Present simulation results for methanol (●) and ethanol (▲) are compared to experimental data (○) and (△) [21]

Table 5. Density and self-diffusion coefficient for the mixture methanol(1) + ethanol(2) at 298.15 K and 0.1 MPa from present molecular dynamics simulations. The number in parenthesis indicates the statistical uncertainty in the last digit

x_1	ρ	D_1	D_2
mol/mol	1/mol	$10^{-9} \text{m}^2/\text{s}$	$10^{-9} \text{m}^2/\text{s}$
0	27.02	—	1.11(2)
0.14	26.22	1.38(2)	1.12(1)
0.30	25.63	1.52(1)	1.25(1)
0.50	25.14	1.73(1)	1.44(1)
0.57	24.81	1.82(1)	1.53(1)
0.75	24.51	2.07(1)	1.72(2)
0.80	23.91	2.14(2)	1.82(2)
0.89	23.58	2.28(1)	1.90(2)
1	23.21	4.95(3)	—

for both alcohols. The present simulation results overestimate slightly the self-diffusion of both alcohols by 5% on average. Furthermore, the predicted data reproduces the composition dependence of both self-diffusion coefficients.

4 Computing Performance

All MD simulations were carried out on the NEC SX-8 with the MPI based molecular simulation program *ms2* developed in our group. The parallelization of the MD part of *ms2* is based on Plimpton's particle-based decomposition algorithm [22].

A typical MD simulation on the NEC SX-8 using one node with 8 processors is compared here to simulations on two other platforms available on our institute. Firstly, LEO, a workstation with 4 dual core Opteron 8216 processors, was considered and secondly, S11, a workstation with 2 Athlon MP 2800+ processors. In all cases, the same simulations were carried out with 864 methanol molecules in the liquid state over 100.000 time steps. It should be noted that for transport properties, as presented in section 3, typically 2.000.000 time steps have to be performed. The comparison is presented in Table 6. As can be assumed, both NEC SX-8 and LEO are much faster than the Athlon based workstation. Nevertheless, it can be confirmed that NEC SX-8 is clearly the most suited platform for MD.

Table 6. Run time on NEC SX-8, LEO and S11 simulating 864 methanol molecules over 100.000 time steps

System	run time
	minutes
NEC SX-8	30
LEO	55
S11	447

References

1. W.E. Nagel, W. Jäger, M. Resch: High Performance Computing in Science and Engineering '05. Springer, Berlin (2005).
2. T. Schnabel, J. Vrabec, H. Hasse: Henry's law constants of methane, nitrogen, oxygen and carbon dioxide in ethanol from 273 to 498 K. *Fluid Phase Equilib.*, **233**, 134 (2005).
3. T. Schnabel, J. Vrabec, H. Hasse: Erratum to "Henry's law constants of methane, nitrogen, oxygen and carbon dioxide in ethanol from 273 to 498 K". *Fluid Phase Equilib.*, **239**, 125 (2006).
4. T. Schnabel, M. Cortada, J. Vrabec, S. Lago, H. Hasse: Molecular Model for Formic Acid adjusted to Vapor-Liquid Equilibria. *Chem. Phys. Lett.*, **435**, 268 (2007).
5. T. Schnabel, B. Eckl, Y.-L. Huang, J. Vrabec, H. Hasse: Molecular Modeling of Hydrogen Bonding Fluids: Formic Acid and Ethanol + R227ea. in W.E. Nagel,

- W. Jäger, M. Resch, High Performance Computing in Science and Engineering '07. Springer, Berlin (2007).
6. D.K. Dysthe, A.H. Fuchs, B. Rousseau: Fluid Transport properties by equilibrium molecular dynamics. I. Methodology at extreme fluid states. *J. Chem. Phys.*, **110**, 4047 (1999).
 7. M.W. Schmidt, M.W. Baldrige, J.A. Boatz, et al.: General atomic and molecular electronic structure system. *J. Comput. Chem.*, **14**, 1347 (1993).
 8. DIPPR Project 801 - Full Version. Design Institute for Physical Property Data/AIChE, 2005.
 9. J. Stoll: Molecular Models for the Prediction of Thermophysical Properties of Pure Fluids and Mixtures, Fortschritt-Berichte VDI, Reihe 3, 836, VDI Verlag, Düsseldorf, (2005).
 10. M.S. Green: Markoff Random Processes and the Statistical Mechanics of Time-Dependant Phenomena 2. Irreversible Processes in Fluids. *J. Chem. Phys.*, **22**, 398 (1954).
 11. R. Kubo: Statistical-Mechanical Theory of Irreversible Processes I. General Theory and Simple Applications to Magnetic and Conduction Problems. *J. Phys. Soc. Jpn.*, **12**, 570 (1957).
 12. P.A. Johnson, A.L. Babb: Liquid Diffusion in Non-electrolytes. *Chem. Rev.*, **56**, 587 (1956).
 13. F.A.L. Dullien: Predictive Equations for Self-Diffusion in Liquids: a Different Approach. *AIChE Journal*, **18**, 62 (1972).
 14. R.L. Hurler, A.J. Eastel, L.A. Woolf: Self-diffusion in monohydric Alcohols under Pressure. *J. Chem. Soc. Far. Trans*, **81**, 769 (1985).
 15. N. Karger, T. Vardag, H.D. Lüdemann: Temperature dependence of self-diffusion in compressed monohydric alcohols. *J. Chem. Phys.*, **93**, 3437 (1990).
 16. N. Asahi, Y. Nakamura: Nuclear magnetic resonance and molecular dynamics study of methanol up to supercritical region. *J. Chem. Phys.*, **109**, 9879 (1998).
 17. S. Meckl, M.D. Zeidler: Self-diffusion measurements of ethanol and propanol, *Mol. Phys.*, **63**, 85 (1988).
 18. J. Alonso, F.J. Bermejo, M. Garcia-Hernandez, J.L. Martinez, W.S. Howells: H-Bond in methanol: a molecular dynamics study. *J. Mol. Struct.*, **250**, 147 (1991).
 19. P.J. Michels, N.J. Trappeniers: Molecular Dynamics calculations of the self-diffusion coefficient below the critical density, *Chem. Phys. Lett.*, **33**, 195 (1975).
 20. P. Sindzingre, M.L. Klein: A molecular dynamic study of methanol near the liquid-glass transition. *J. Chem. Phys.*, **95**, 4681 (1992).
 21. P.A. Johnson, A.L. Babb: Self-diffusion in liquids. I. Concentration dependence in ideal and non-ideal binary solutions, *J. Chem. Phys.*, **60**, 14 (1956).
 22. S. Plimpton: Fast Parallel Algorithms for Short-Range Molecular Dynamics. *J. Comp. Phys.*, **117**, 1 (1994).